

Analysis of Fission Reaction Rate Distributions for the BFS-84-1 Experiments

Sunghwan Yun* and Jae-Yong Lim

Korea Atomic Energy Research Institute (KAERI)
989-111 Daedeok-daero, Yuseong-gu, Daejeon, Korea, 305-353

*Corresponding author: syun@kaeri.re.kr

1. Introduction

The Korea Atomic Energy Research Institute (KAERI) has been developing a Prototype Gen-IV Sodium-cooled Fast Reactor (PGSFR), in which blanket-free U-Zr metallic fuelled core concept is adopted, to aim at design approval [1, 2].

To achieve design approval of the PGSFR, proof of the fuel integrity during operation is one of the essential work. At the view point of core neutronics design, validation of the power distribution is one part of this proof. Hence, we performed a Mock-up physical experiment of the PGSFR (named as BFS-84-1 experiment) by collaborating with Russian IPPE, which includes measurements of fission reaction rate distribution to validate power distribution [3].

In this paper, the fission reaction rate distributions measured at the BFS-84-1 experiment are analyzed by using as-built MCNP model [4, 5] and ENDF/B-VII.0 library [6].

2. BFS-84-1 Experiment

The BFS-84-1 critical assembly is composed of dual enrichment uranium metal-fueled core surrounded by a steel reflector. Two enrichment zones consist of a 15.9 wt.% enriched Inner Core (IC) zone and 16.8 wt.% enriched Outer Core (OC) zone to describe a four batch inner core and five batch outer core in the PGSFR [7]. Axially, the core is surrounded by a lower steel reflector and sodium/gas plenum as described in the reference [8].

The radial and axial configuration of the BFS-84-1 experiment are described in Figs. 1 and 2, respectively.

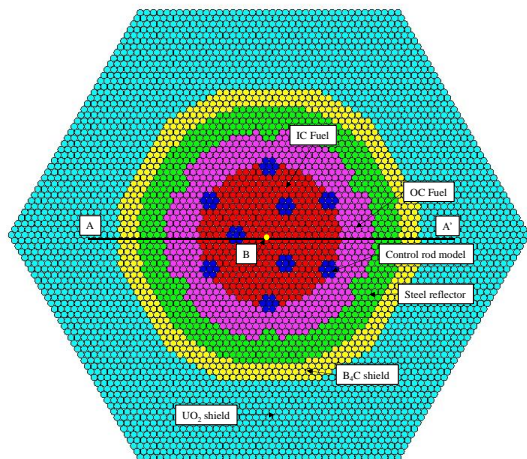


Fig. 1. Radial configurations for the BFS-84-1 critical assembly

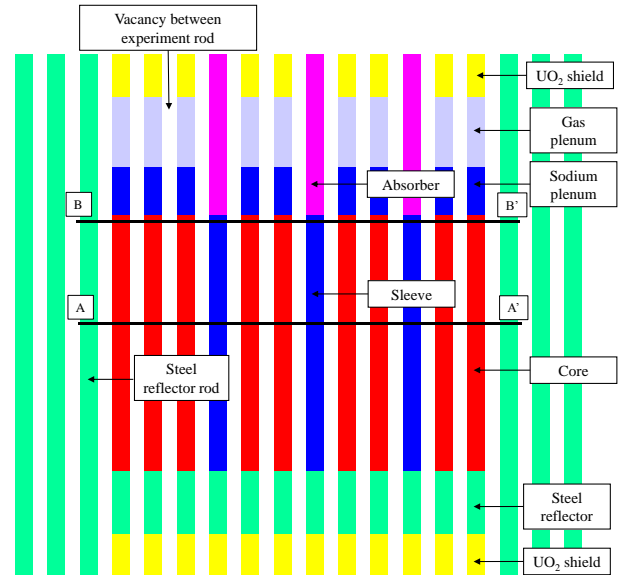


Fig. 2. Axial configurations for the BFS-84-1 critical assembly

Fission reaction rate distributions were measured by inserting small size fission chamber into the gap between experiment rods. Since the small size fission chamber was coated by U-235, U-238, and Pu-239, fission reaction rates can be measured at both of fuel and non-fuel regions.

Radial fission reaction rate distributions were measured at positions along AA' line and axial fission reaction rate distributions were measured at position B in the Fig. 1. Axially, radial fission reaction rate distributions were measured at both of core center position (AA' line in Fig. 2) and core top position (BB' line in Fig. 2) as shown in Fig. 2. For radial fission reaction rate distribution measurements, the measurement results at core top region will represent the error of power distribution due to control rod insertion.

During the measurement of the radial fission reaction rate distributions, some positions were not measured due to existence of BFS facility safety system.

3. Results of fission reaction rate distributions

3.1 Radial fission reaction rate distributions

Calculation to Experimental values for U-235, Pu-239, and U-238 radial fission reaction rates are shown in Fig. 3 through Fig. 5, respectively. In addition, tables I and II show averaged error of radial fission reaction

rate at core region and steel reflector region, respectively.

For all of U-235, Pu-239, and U-238 fission reaction rates at core region, calculation results show good agreement with experimental results. The averaged errors of U-235 and Pu-239 fission reaction rates are within 1σ range at both of core central and core top region. Hence we can conclude that there is negligible error in power distribution estimation using ENDF/B-VII.0 library.

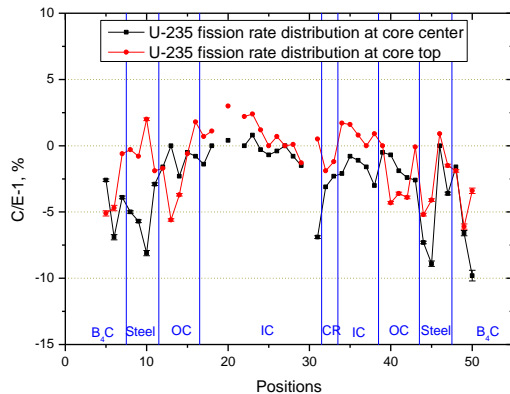


Fig. 3. Radial U-235 fission reaction rate distributions

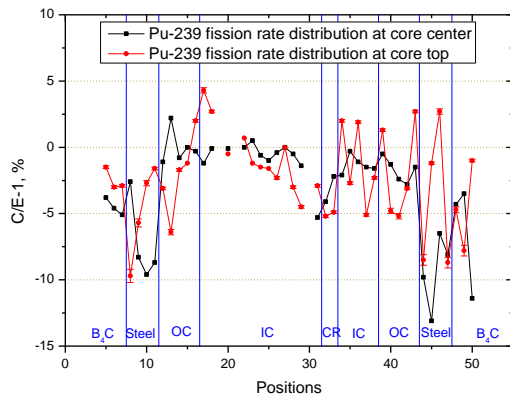


Fig. 4. Radial Pu-239 fission reaction rate distributions

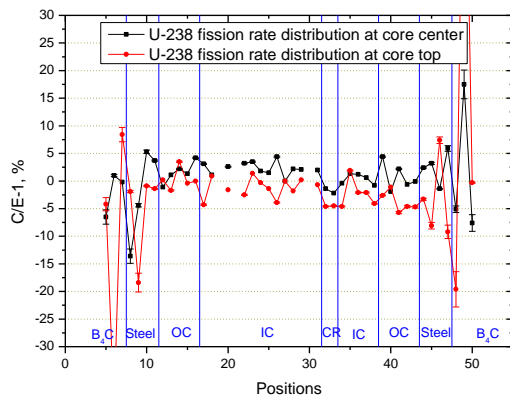


Fig. 5. Radial U-238 fission reaction rate distributions

Table I: Averaged error of radial fission reaction rate distributions at core region, %

	Core center	Core top
U-235	-1.3 ± 1.5	-0.3 ± 2.2
Pu-239	-1.1 ± 1.4	-1.6 ± 2.9
U-238	1.3 ± 1.9	-1.8 ± 2.3

Table II: Averaged error of radial fission reaction rate distributions at steel reflector region, %

	Core center	Core top
U-235	-5.2 ± 3.0	-1.4 ± 2.4
Pu-239	-8.3 ± 3.0	-4.4 ± 4.4
U-238	0.1 ± 6.5	-4.5 ± 7.6

3.2 Axial fission reaction rate distributions

Calculation to Experimental values for axial fission reaction rates are shown in Fig.6 and region-wise averaged error of axial fission reaction rates are shown in table III.

Similar to the previous radial fission reaction rate distributions, calculation results for all of fission reaction rates at core region show good agreement with experimental results within 1σ range.

However, for the lower steel reflector region, calculation results of Pu-239 and U-235 fission reaction rates show $\sim 10\%$ overestimation while calculation results of U-238 fission reaction rates show $\sim 10\%$ underestimation. In contrast, for sodium plenum region, calculation results of Pu-239 and U-235 fission reaction rates show $\sim 10\%$ underestimation. For gas plenum region, due to large measurement uncertainty, it is difficult to confirm tendency of results.

Although underestimations or overestimations of fission reaction rates at non-fuel regions do not influence to the error of power distribution, these results may be valuable for the future cross-section development.

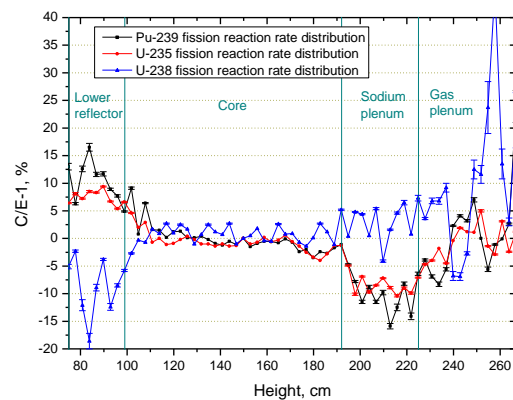


Fig. 6. Axial fission reaction rate distributions

Table III: Averaged error of axial fission reaction rate distributions, %

	Lower reflector	Core	Sodium plenum	Gas plenum
Pu-239	10.0±3.8	-0.1±2.4	-10.1±3.4	0.8±8.1
U-235	7.5±1.3	-0.6±1.7	-8.4±1.7	-0.6±3.0
U-238	-9.1±5.3	0.8±1.6	2.9±3.4	10.1±13.6

5. Conclusions

In this paper, radial and axial fission reaction rates of U-235, Pu-239, and U-238 isotopes, measured at the BFS-84-1 experiment, are analyzed using the MCNP6 code and ENDF/B-VII.0 library on a framework of validating power distributions of the PGSFR core.

For all fission reaction rates at core region, calculation results show good agreement with experimental results within 1 σ range. Since the fission power distribution at PGSFR is mostly originated from U-235, U-238, and Pu-239 isotopes, we can conclude that there will be no significant bias in power distribution of the PGSFR core when ENDF/B-VII.0 library and precise MCNP model were used to calculate fission power distributions.

In addition, considerable error of fission reaction rates at non-fuel regions are also reported. These data may be useful for improvement of the cross-section library using cross-section adjustment method or re-evaluation method.

ACKNOWLEDGEMENTS

The authors are grateful to Dr. M. Semenov, Dr. G. Mikhailov and colleagues in the IPPE for collaborating KAERI's physical experiment programs.

This work was supported by a National Research Foundation of Korea (NRF) grant funded by the Korean government (MSIP) (No. NRF-2012M2A8A2025622).

REFERENCES

- [1] H. K. Joo, et.al., Status of the fast reactor technology development in Korea, The 48th TWG-FR Meeting, Obninsk, May 25–29, (2015).
- [2] J. Yoo, et.al., Overall System Description and Safety Characteristics of Prototype Gen IV Sodium Cooled Fast Reactor in Korea, Nuclear Engineering and Technology, Vol. 48, p. 1059, (2016).
- [3] G. M. Mikhailov et al., Results of Experimental Studies of Neutronic Characteristics at the Critical Assembly-PGSFR Reactor Model, IPPE, 2016.
- [4] D. B. Pelowitz, et.al., MCNP6TM User's Manual, LA-CP-13-00634, LANL, May (2013).
- [5] S. Yun, Assessment of the BFS-84-1 Physical Experiment, SFR-111-DR-486-040.Rev00, KAERI, 2016.
- [6] M. B. Chadwick, et al., ENDF/B-VII.0: Next Generation Evaluated Nuclear Data Library for Nuclear Science and Technology Nuclear Data Sheets, Vol. 107, p. 2931, doi: 10.1016/j.nds.2006.11.001, 2006.

[7] J.-Y. Lim, et. al., PGSFR Core Design and Performance Characteristics, Transactions of the American Nuclear Society, Vol. 114, p. 700, (2016).

[8] S Yun and J.-Y. Lim, Prediction of the Sodium Void Reactivity in the Metal-fueled SFR, Transactions of the Korean Nuclear Society Autumn Meeting Gyeongju, Korea, October 27-28, 2016.